# Adsorption behavior of surfactants on lignite particles with different densities in aqueous medium

# Jie Wang[*], Yaqun He[*,**], Baofeng Wen[*], Xiangyang Ling[*], Weining Xie[*], Shuai Wang[*]

[*]  School of Chemical Engineering and Technology, China University of Mining and Technology, Xuzhou, Jiangsu 221116, China
[**] Advanced Analysis and Computation Center, China University of Mining and Technology, Xuzhou, Jiangsu, 221116, China. Corresponding author: yqhe_cumt@126.com (Yaqun He)

**Abstract:** Lignite is well known for its strong hydrophilicity and hard-to-float properties. However, the surface free energy of the solid is made up of two components, that is the Lifshitz-van der Waals and acid-base interaction energy. Differences in these two components between the low ash (lower density) and high ash fraction (higher density) provide a benefit for improving the separation efficiency through introducing surfactants in flotation. In this paper, thermodynamic characterization of three density lignite fractions was measured by a Washburn dynamic method. Combining the Washburn equation and Van Oss-Chaudhury-Good theory, the surface free energy components of three samples were calculated according to the wetting process by n-hexane, diiodomethane, deionized water and ethylene glycol. The Lifshitz-van der Waals part of surface free energy reduced with the coal density increase, especially between fractions of -1.45 g/cm$^3$ and 1.45-1.80 g/cm$^3$, while the Lewis base part increased slightly. The interfacial interaction free energies between the surfactant and lignite in aqueous medium indicated that the low hydrophilic index benefited for the stronger adsorption intensity. Increase of the surfactant Lifshitz-van der Waals component increases the adsorptive intensity on lower density lignite and the repulsive intensity on higher density lignite, which is beneficial for separation.

*Keywords: interfacial surface free energy, adsorption, lignite, surfactant, Washburn equation*

## Introduction

Lignite is well known for its strong hydrophilicity and hard-to-float properties. In aqueous media, the mineral-rich particles in lignite are also hydrophilic. In practice, surfactants have been applied to pretreat coal samples to adjust the surface hydrophobicity of the coal-rich or mineral-rich particles. Cationic surfactants have been proved to have an essential function in reverse flotation of hard-to-float coal, such as either lignite or oxidized coal (Wen and Sun 1977; Sarikaya and Özbayoğlu

1995; Zhang and Liu 2015). A large number of nonionic surfactants has been used to investigate the flotation efficiency more widely (Celik and Yoon 1991; Vamvuka and Agridiotis 2001; Zhang and Tang 2013). Surfactants can play a role of either frother, collector or both. The frother may act as collector when the coal surface has some polar moieties. Although, it is clear that inorganic silicate minerals have the high-energy surface subject to facilitate strong adsorption by the cationic surfactant, such as fatty amine (Wen and Sun 1977; Xia and Yang 2013), the adsorption behavior of nonionic surfactant on coal-rich/mineral-rich lignite particles is still unclear. This work is mainly focused on the interfacial interaction free energies between low molecular weight non-ionic surfactants and low ash (lower density) or high ash (higher density) fractions of Inner Mongolia lignite. Low rank lignite is characterized by more oxygen functional groups on the particle surface, which results in the hydrophilicity of lignite. However, the minerals are mainly hydrophilic silicates, carbonates, sulfates and quartz.

In terms of the interfacial interaction free energy, it is essential to confirm surface free energy components of the lower/higher density lignite samples. Van Oss-Chaudhury-Good theory indicates that the total surface free energy of substance is composed of the non-polar (Lifshitz-van der Waals $\gamma^{LW}$) and polar parts (Lewis acid-base, $\gamma^+$ and $\gamma^-$) (Van Oss et al., 1979; Van Oss et al., 1980; Van Oss, 2006). Using the combined Washburn equation (Grundke et al., 1996; Chau 2009), the surface free energy and their polar/non-polar components of the low and high ash lignite can be determined. Zou et al. (2013) investigated the surface free energy components of two fine liberated middling bituminous coals through such method. The surface free energy components of coals are consistent with the regressive release flotation test results. The calculated interfacial interaction free energy is concerned with the surface free energy components of solid and surfactant. Wang et al. (2011) studied the surface free energy components of frothers through contact angle measurements. Based on the measured surface free energy components of the solids and surfactants, their interaction free energies were calculated.

In this paper, the raw lignite particles (-0.5 mm) were separated into three densities, including -1.45 g/cm$^3$, 1.45-1.80 g/cm$^3$ and +1.80 g/cm$^3$ fractions. The surface functional group compositions were determined by FTIR. n-hexane with low surface tension of 18.4 mN·m$^{-1}$ was the probe to measure the geometric factor of packed powder beds. Other three types of probe liquids, including two polar (deionized water and ethylene glycol) and one non-polar (diiodomethane), were used in the Washburn wetting tests in order to calculate their contact angles. All the contact angle measurements were performed at 20 °C. The surface free energy of different density lignite samples was determined. Furthermore, the relationship between the surface chemical structure and surface free energy of three lignite samples was discussed. Based on the results, the interfacial free energy between the surfactant and lignite surface in the aqueous medium was calculated. In addition, the effect of reagent structure on different adsorption behaviors was also concerned.

## Materials and methods

### Materials

A lignite sample was obtained from Inner Mongolia Province, China. Sink and float tests for the fine fraction (-0.5 mm) were carried out in dense medium liquids with densities of 1.45 and 1.8 g/cm$^3$, respectively. After sink and float separation, each product was washed, rinsed and dried at 105 °C for 6 h in a vacuum oven. Samples of the products were weighed and then ground to -74 μm separately to determine their ash content and wetting behavior.

The probe liquids, including n-hexane, ethylene glycol, deionized water and diiodomethane were of analytical purity. Surfactants, including terpineol (TP), methyl isobutyl carbinol (MIBC), tripropylene glycol n-butyl ether (TPnB) and diethyl o-phthalate (DOP) were also of analytical purity.

### Methods

#### Contact angle measurement

A KRUSS tensiometer K100 was used to measure the contact angle of coal samples with various densities in different liquids. Temperature was kept strictly around 20 ± 0.5 °C. A small round-shape filter paper was placed at the bottom of the Washburn tube. Different density fractions of 2.0000 g was weighed and put into a clean Washburn tube. Then Washburn tube was fixed on the hook of the Tensiometer K100. A 30 cm$^3$ probe liquid rose slowly until about 2 mm from the bottom of the tube. Before the measurement, the physical parameters of the probe liquid, including density $\rho$, surface tension $\gamma$ and liquid viscosity $\eta$, were inserted in the measuring process. With the surface of liquid got in touch with the bottom of the tube automatically, the tensiometer started to record the mass increment $w$ with the contact time $t$ with the set of 200 s.

According to the Washburn equation, inserted in measuring software, the contact angle can be obtained from the slope of $w^2 - t$:

$$w^2 = c \frac{\rho^2 t}{\eta} \gamma_1 \cos\theta \tag{1}$$

where $c$ is the geometric factor of the packed bed, $c = R_{eff} \varepsilon^2 \left(\pi r^2\right)^2$ $R_{eff}$ (μm) is the effective radius of capillary, $\varepsilon$ is the porosity, $r$ (mm) is the radius of packed bed, $\rho$ (g·cm$^{-3}$) is the density of the liquid, $\gamma$ (mN·m$^{-1}$) is the surface tension of liquid, $\eta$ (mN·m$^{-2}$·s$^{-1}$) is the liquid viscosity and $\theta$ (°) is the contact angle.

Firstly, the geometric factor $c$ of different density lignite solids was confirmed before contact angle measurement. In the tests, n-hexane was used as the reference liquid (Zou et al., 2013). Therefore, the geometric factor $c$ of the typical density lignite solid can be determined from Eq. (1). In order to obtain the repeatability, the geometric factor $c$ of each solid sample was tested twice. Probe liquids used in the

experiment were n-hexane, ethylene glycol, deionized water and diiodomethane. The parameters of the surface free energy of these liquids are shown in Table 1 (Li et al., 1993; Iveson et al., 2000).

Table 1. Physical parameters of probe liquids at 20 °C

| Probe liquid | $\rho$ g/cm$^3$ | $\eta$ mPa·s | $\gamma_l$ | $\gamma_l^{LW}$ | $\gamma_l^+$ | $\gamma_l^-$ |
|---|---|---|---|---|---|---|
| n-hexane | 0.661 | 0.326 | 18.4 | 18.4 | 0 | 0 |
| deionized water | 0.998 | 1.002 | 72.8 | 21.8 | 25.5 | 25.5 |
| ethylene glycol | 1.109 | 21.81 | 48 | 29 | 1.92 | 47.0 |
| diiodomethane | 3.325 | 2.762 | 50.8 | 50.8 | 0 | 0 |

**Calculation of surface free energy**

Van Oss et al. (1980) supposed that the surface free energy of solid/liquid is made up of two components, that is the Lifshitz-van der Waals $\gamma^{LW}$ and the acid-base interaction energy $\gamma^{AB}$, which is composed of Lewis acid component $\gamma^+$ and base component $\gamma^-$. The surface free energy can be expressed as follows:

$$\gamma = \gamma^{LW} + \gamma^{AB} \tag{2}$$

while the relationship between *i* (solid) and *j* (liquid) interface interaction free energy can be expressed as:

$$\Delta G_{ij} = -2(\sqrt{\gamma_i^{LW}\gamma_j^{LW}} + \sqrt{\gamma_i^+\gamma_j^-} + \sqrt{\gamma_i^-\gamma_j^+}) \qquad . \tag{3}$$

The Young equation characterizes the relationship between the solid surface energy $\gamma_S$, liquid surface free energy $\gamma_L$, solid-liquid interaction free energy $\gamma_{SL}$ and the equilibrium contact angle ($\theta$) expressed by a formula:

$$(1+\cos\theta)\gamma_L = -\Delta G_{SL} \tag{4}$$

The relationship between the surface free energy components and their content angle can be expressed as:

$$(1+\cos\theta)\gamma_L = 2\left(\sqrt{\gamma_S^{LW}\gamma_L^{LW}} + \sqrt{\gamma_S^+\gamma_L^-} + \sqrt{\gamma_S^-\gamma_L^+}\right). \tag{5}$$

From the contact angle of three probe liquids on the solids, the surface free energy components of the solids, including Lifshitz-van der Waals $\gamma_s^{LW}$, Lewis acid component $\gamma^+$ and base component $\gamma^-$ can be calculated by using Eq.(5).

The interaction free energy of two-phase, solid and liquid (L) , is expressed by Eq.(3). The interaction free energy of the lignite particles and surfactant in water (W) can be expressed as:

$$\Delta G_{iWj}^{LW-AB} = \Delta G_{iWj}^{LW} + \Delta G_{iWj}^{AB} = 2\left(\sqrt{\gamma_i^{LW}} - \sqrt{\gamma_W^{LW}}\right)\left(\sqrt{\gamma_W^{LW}} - \sqrt{\gamma_j^{LW}}\right)$$
$$+2\left[\sqrt{\gamma_W^+}\left(\sqrt{\gamma_i^-} + \sqrt{\gamma_j^-} - \sqrt{\gamma_W^-}\right) + \sqrt{\gamma_W^-}\left(\sqrt{\gamma_i^+} + \sqrt{\gamma_j^+} - \sqrt{\gamma_W^+}\right) - \sqrt{\gamma_i^+ \gamma_j^-} - \sqrt{\gamma_i^- \gamma_j^+}\right] \quad . \quad (6)$$

## Results and discussion

### Surface functional group analysis

Table 2 shows the ash content of the coal samples with different densities. The FTIR are shown in Fig. 1. The FTIR signals deriving from chemical functional groups are listed in Table 3 (Painter and Snyder 1981; Liang et al., 2015).

Table 2. Ash content of coal samples with different densities

| Coal sample | -1.45 g/cm$^3$ | -1.80+1.45 g/cm$^3$ | +1.80 g/cm$^3$ |
|---|---|---|---|
| Ash content, % | 8.22 | 27.32 | 63.51 |

Table 3. Band assignments for FTIR spectra of coals (Painter and Snyder 1981; Liang et al., 2015)

| Wavenumber (cm$^{-1}$) | Functional groups |
|---|---|
| 3400-3700 | -OH(minerals) |
| 3100-3400 | -OH |
| 3000-3100 | Aromatic CHx stretching |
| 2800-3000 | Aliphatic $CH_x$ stretching |
| 1650-1800 | -COOH |
| 1550-1650 | Aromatic C=C ring stretching |
| 1300-1550 | Aliphatic $CH_x$ bending |
| 1100-1300 | C-O-C stretching |
| 900-1100 | Si-O stretching |
| 650-900 | Aromatics CHx Out-of-plane deformation |
| -650 | Al-O formation, Si-O |

Figure 1 presents the surface functional groups of three different density lignite samples. For the -1.45 g/cm$^3$ coal sample, the wide organic -OH peak occupies a quite high proportion of the coal surface at 3400 cm$^{-1}$. Despite of the wide organic -OH, the absorbance of C=C peak, is presented by the strongest peak at 1600 cm$^{-1}$ (Fig. 1a). Besides, the characteristic peaks of aliphatic $CH_X$ are found at the ranges of 2800 - 3000 cm$^{-1}$ and 1300 -1550 cm$^{-1}$. On the other hand, the comparatively weak peaks of Si-O are also seen at nearly 1000 cm$^{-1}$ and the range of -650 cm$^{-1}$ from the FTIR spectrum of the coal sample -1.45 g/cm$^3$. However, for -1.80 g/cm$^3$+1.45 g/cm$^3$ lignite coal samples, the organic peaks of -OH and C=C are decreased significantly in the comparison with the results presented in Fig. 1a. On the contrary, the mineral peaks of Si-O are increased remarkably at the ranges of 900 -1100 cm$^{-1}$ and -650 cm$^{-1}$. In

addition, -OH peaks at 3400 cm$^{-1}$-3700 cm$^{-1}$ are presented alongside the organic -OH. From Figure 1c, the organic peaks are further decreased for +1.80 g/cm$^3$ lignite sample, while the inorganic peaks are increased remarkably. The absorbance of the inorganic peaks are much higher than the organic peaks.
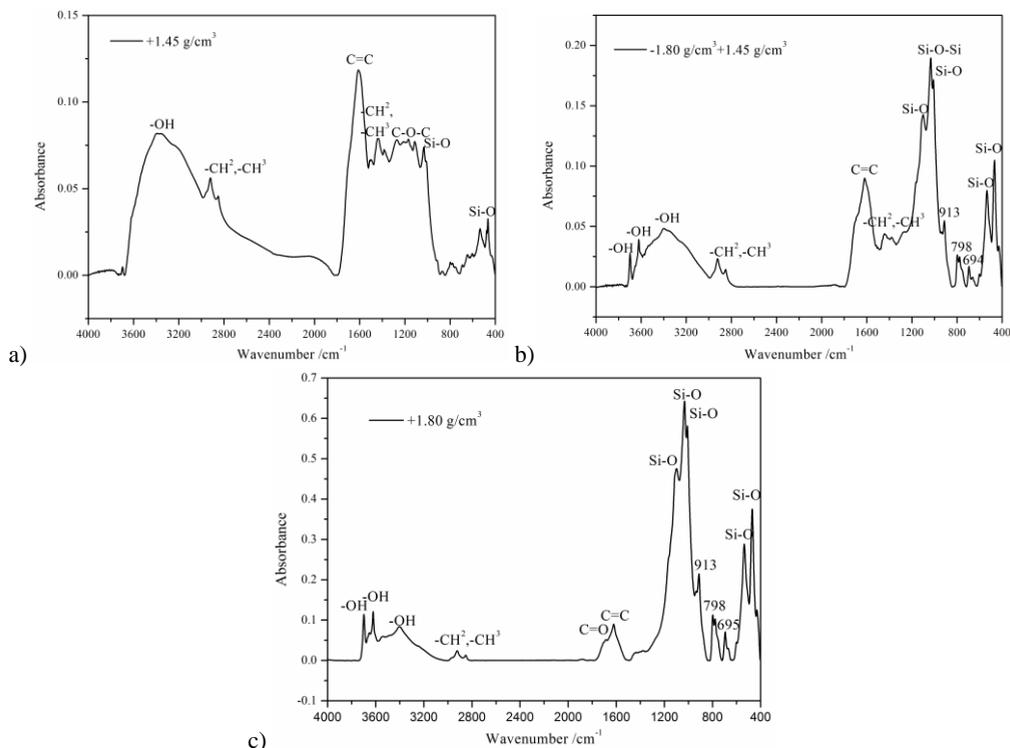


Fig. 1. FTIR of three density lignite coal samples, (a) -1.45 g/cm$^3$, (b) -1.80 + 1.45 g/cm$^3$, (c) +1.80 g/cm$^3$

## Contact angle and surface free energy calculation

Table 4 shows the average geometric factor *c* and contact angle between the probe liquid and lignite from the Washburn method. For the -1.45 g/cm$^3$ lignite sample, the contact angles were 60, 65 and 87° for diiodomethane, ethylene glycol and deionized water, respectively. From the physical parameters, shown in Table 1, the polarity of deionized water is stronger than that of ethylene glycol. It is shown that non-polar diiodomethane can wet the lower density lignite easily, while more polar deionized water spreads more difficultly than ethylene glycol. For +1.45-1.80 g/cm$^3$ lignite, the contact angles were 70, 68 and 86° for diiodomethane, ethylene glycol and deionized water, respectively. The deionized water spreads on the +1.45-1.80 g/cm$^3$ lignite with more difficulty than non-polar diiodomethane. In the case of the +1.80 g/cm$^3$ lignite, the wetting phenomenon was similar with that of the +1.45-1.80 g/cm$^3$ lignite sample. On the other hand, diiodomethane and ethylene glycol wet the lignite more easily with

the decrease of lignite sample density, while deionized water wets lignite more difficult. In conclusion, with the polarity increase of the probe liquid, the contact angle increases obviously for the lower density lignite. However, for the medium and the higher density coal samples, the medium polar liquid wets two samples more easily than the non-polar/ strong polar liquid.

Table 4. Geometric factor $c$ and contact angle of lignite samples with different densities

| lignite density, $\rho$ (g·cm⁻³) | $c$ (10⁻⁶ cm⁻⁵) | Contact angle, $\theta$ (°) | | | |
|---|---|---|---|---|---|
| | | n-hexane | diiodomethane | ethylene glycol | deionized water |
| -1.45 | 2.16 | 0 | 60 | 65 | 87 |
| +1.45-1.80 | 2.17 | 0 | 70 | 68 | 86 |
| +1.80 | 1.42 | 0 | 75 | 74 | 85 |

By combining the parameters given in Tables 2 and 4, the surface free energy components of the lignite samples can be calculated from Eq. (5), and the results are listed in Table 5.

Table 5. Surface free energy components of lignite samples with different densities (mN/m)

| lignite density, $\rho$ (g·cm⁻³) | $\gamma_S^{LW}$ | $\gamma_S^+$ | $\gamma_S^-$ | $\gamma_S^{AB}$ | $\sqrt{\gamma_S^+}+\sqrt{\gamma_S^-}$ * | $\gamma_S$ |
|---|---|---|---|---|---|---|
| -1.45 | 28.58 | 0.0289 | 7.83 | 0.95 | 2.97 | 29.53 |
| +1.45-1.80 | 22.87 | 0.2304 | 7.54 | 2.64 | 3.23 | 25.51 |
| +1.80 | 20.12 | 0.0841 | 9.89 | 1.82 | 3.43 | 21.94 |

* $\sqrt{\gamma_l^+}+\sqrt{\gamma_l^-}$ is hydrophilic index (Wang et al., 2011).

From the results shown in Table 5, it is indicated that the main surface free energy component for the -1.45 g/cm³ density lignite is Lifshitz-van der Waals $\gamma^{LW}$. The Lewis acid component $\gamma_S^+$ is comparatively low and equal to 0.0289 mN/m, while the base component is 7.83 mN/m. Similar values of the Lewis acid $\gamma_S^+ s$ and base $\gamma_S^-$ components are shown in Table 5 for +1.45 g/cm³ and +1.80 g/cm³ fractions. Besides, the Lifshitz-van der Waals $\gamma^{LW}$ is found to be the main component in the medium and high density lignite samples. However, the Lifshitz-van der Waals $\gamma^{LW}$ decreases with the increase of the lignite density, which indicates that the non-polarity of lower density lignite is stronger than that of the higher density sample. The Lewis acid components $\gamma_S^+$ are small for all the three density samples, while the Lewis base component $\gamma_S^-$ increases for the +1.80 g/cm³ coal sample. The Lewis acid-base components $\gamma_S^{AB}$ of lignite show no clear regularity. However, the hydrophilic index $\sqrt{\gamma_S^+}+\sqrt{\gamma_S^-}$ increases with the density increase. The surface free energy demonstrates

the decreasing trend with the increase of the density due to the absolute predominance of the Lifshitz-van der Waals component. By combining the results of the surface functional groups shown in Fig. 1, it is concluded that the inorganic oxygen functional groups have the stronger hydrophilicity than the organic oxygen groups.

### Interfacial interaction free energy in aqueous medium

The surface tension parameters and hydrophilic index $\sqrt{\gamma_l^+}+\sqrt{\gamma_l^-}$ of four types of surfactants, including TPnB, DOP, TP and MIBC are listed in Table 6 (Wang et al., 2011).

Table 6 Surface free energy components of surfactants

| Surfactant | $\gamma_l$ | $\gamma_l^{LW}$ | $\gamma_l^+$ | $\gamma_l^-$ | $\sqrt{\gamma_l^+}+\sqrt{\gamma_l^-}$ | Chemical structure |
|---|---|---|---|---|---|---|
| TP | 31.19 | 30.64 | 0.019 | 3.97 | 2.13 | |
| MIBC | 26.79 | 26.44 | 0.023 | 1.34 | 1.31 | |
| TPnB | 33.17 | 32.08 | 0.032 | 9.33 | 3.23 | |
| DOP | 37.89 | 36.82 | 0.044 | 6.46 | 2.75 | |
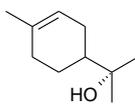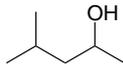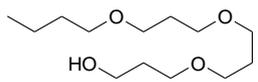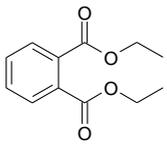
From Table 6, there is a notable positive correlation between the number of carbon atoms in the reagent molecule and the Lifshitz-van der Waals component $\gamma_l^{LW}$. Besides, the aromatic ring enhances the Lifshitz-van der Waals component $\gamma_l^{LW}$ of DOP than that of TPnB despite the number of carbon atoms of the former is less than that of the latter. In general, the hydrophilic index increases with the increase of the number of oxygen atoms in the reagent molecule (Table 6). However, the hydrophilic indexes are different though the same four oxygen atoms in the TPnB and DOP molecule. In details, three ether bonds and one hydroxyl are in TPnB, while two ester groups are formed in DOP. Hence, ether bond and hydroxyl are more hydrophilic than the ester group in the reagent molecule. For the molecules of TP and MIBC, one hydroxyl is shown in each molecule, but their hydrophilic indexes are also different. Therefore, the cyclic structure results in the more hydrophilic property of TP than that of MIBC. In conclusion, not only the number of oxygen atoms and structure of

oxygenated groups but also the chemical structure of hydrocarbon have significant influence on the hydrophilic index of non-ionic surfactants.

The adsorption performance of tested reagents on different density lignite samples are characterized by their calculated interaction free energy (Eq. 6). The results are shown in Figure 2 to 4.
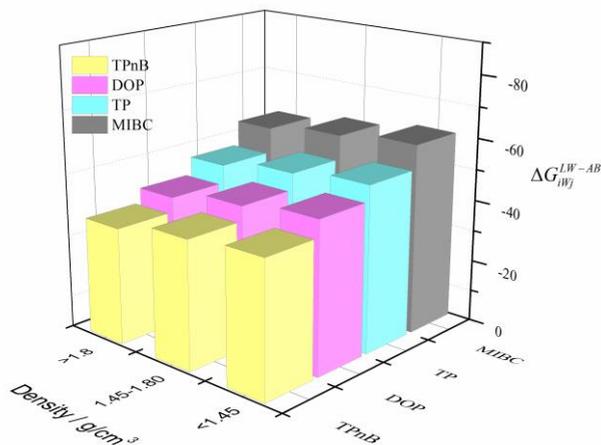


Fig. 2. Total interaction free energy $\Delta G_{iWj}^{LW-AB}$
between surfactant and lignite in aqueous medium

From Figure 2, it is shown that different types of surfactants adsorb on lignite samples with various densities with different intensities. For the fraction of -1.45 g/cm$^3$, the total interaction free energies are -42.75, -48.17, -53.13 and -60.68 mJ/m$^2$ for TPnB, DOP, TP and MIBC, respectively. Similarly, the total interaction free energies for other two samples display the increasing trend for four surfactants in the above order. The typical values are -40.90, -45.54, -50.77 and -58.25 mJ/m$^2$ for the medium density lignite sample and -37.19, -41.80, -47.50 and -55.54 mJ/m$^2$ for +1.80 g/cm$^3$ lignite. The negative values of these interaction free energies indicate that the adsorption processes are spontaneous. Obviously, the adsorption intensities of these surfactants are in the order MIBC > TP >DOP >TPnB for three density samples. On the other hand, the surfactant adsorbs on the lignite surface more easily and strongly with the decrease of particle density. Since the total interaction free energy is consisted of the Lifshitz-van der Waals and Lewis acid-base component, it is necessary to separate it to these two parts in order to distinguish their effects.

Figure 3 shows the Lewis acid-base interaction free energy $\Delta G_{iWj}^{AB}$ between the surfactant and lignite in the aqueous medium. Apparently, the trend in Fig. 3 is similar with that in Fig. 2. For the -1.45 g/cm$^3$ lignite sample, Lewis acid-base interaction free energies are -41.41, -46.27, -51.96 and -60.04 mJ/m$^2$ for TPnB, DOP, TP and MIBC, respectively. On the other hand, the Lewis acid-base interaction free energies for the

other two samples are -40.68, -45.22, -50.57 and -58.14 mJ/m$^2$ for the medium density lignite and -37.55, -42.32, -47.82 and -55.71 mJ/m$^2$ for the higher density lignite samples for TPnB, DOP, TP and MIBC, respectively. Comparison of the total interaction free energy with Lewis acid-base interaction free energy shows that the absolute value of each sample is decreased slightly for the density fractions of -1.45 g/cm$^3$ and +1.45-1.80 g/cm$^3$, while it increases slightly for the +1.80 g/cm$^3$ lignite. Hence, the Lewis acid-base interaction plays a dominant role in the adsorption performance of these non-ionic surfactants on the lignite surface in the aqueous medium.
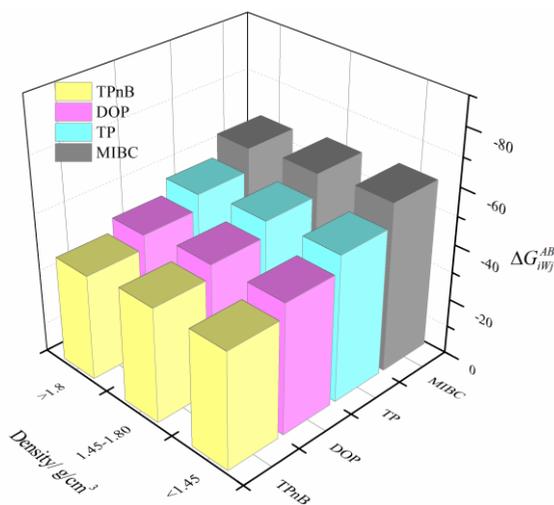


Fig. 3. Lewis acid-base interaction free energy $\Delta G_{iWj}^{AB}$ between surfactant and lignite in aqueous medium

Figure 4 shows the Lifshitz-van der Waals interaction free energy between surfactant and lignite in the aqueous medium. Firstly, it is quite different from the circumstances in Figs. 2 and 3. For the fraction of -1.45 g/cm$^3$, Lifshitz-van der Waals interaction free energies are -1.35, -1.89, -1.17 and -0.64 mJ/m$^2$ for TPnB, DOP, TP and MIBC, respectively. For the other two coal samples, the typical values are -0.23, -0.32, -0.20 and -0.11 mJ/m$^2$ for the medium density lignite and 0.37, 0.51, 0.32 and 0.17 mJ/m$^2$ for the higher density lignite. The absolute values of these interaction free energies are much smaller than Lewis acid-base interaction free energies, which indicates the comparatively weak interaction of Lifshitz-van der Waals. On the other hand, these interaction energies for the higher density lignite are all positive, which means the repulsive Lifshitz-van der Waals force between the surfactant and higher density lignite in aqueous medium. In addition, larger Lifshitz-van der Waals force is observed obviously in the lower density than that in the medium density.
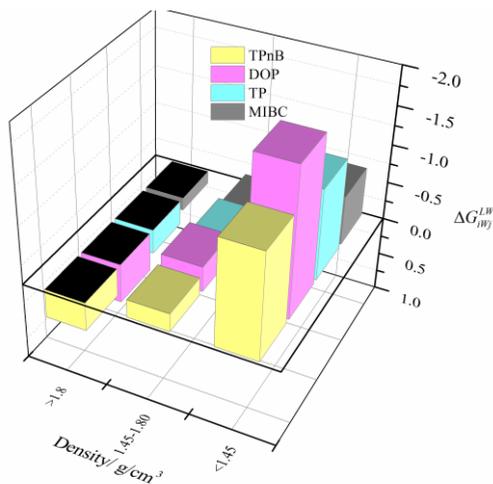
Fig. 4 Lifshitz-van der Waals interaction free energy $\Delta G_{iWj}^{AB}$
between surfactant and lignite in aqueous medium

A schematic diagram of interfacial interaction between non-ionic surfactant and particle in water is shown in Fig. 5. The models of lower and higher density lignite particle surfaces are derived from the FTIR analysis (Figs. 1a and 1c). From the above results, two components of the interaction between surfactant and lower density lignite are both attractive in the aqueous medium, while the Lifshitz-van der Waals interaction is repulsive for higher density lignite. This repulsive interaction between surfactant and higher density lignite surface results in the adsorption priority to the lower density sample for the non-ionic surfactant. For the Lewis acid-base interaction free energy (Fig. 3), MIBC, with the smallest hydrophilic index, presents relatively stronger adsorption intensity on the lignite surfaces. Among the other three reagents, this adsorption intensity component decreases with the increase of the hydrophilic index. In addition, the Lewis acid-base interaction intensity increases slightly with the decrease of the lignite hydrophilic index (Fig. 3). Therefore, the low hydrophilic index, regardless of surfactant or lignite, benefits for the Lewis acid-base interaction intensity. However, the Lifshitz-van der Waals interaction intensity shows a positive relationship with the Lifshitz-van der Waals components of surfactants for the lower and medium density lignite samples. For the higher density lignite samples, larger Lifshitz-van der Waals components of surfactants lead to the stronger repulsive intensity. In conclusion, the non-ionic surfactant has the priority to adsorb on the lower density lignite coal particle surfaces, which benefits for improving the hydrophobicity of the lower density lignite coal. Besides, to increase the adsorption difference, the surfactant should increase the Lifshitz-van der Waals component but decrease the Lewis acid-base component.
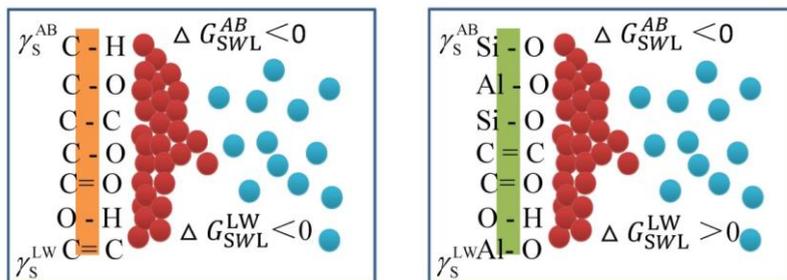
Fig. 5. Schematic diagram of interfacial interaction between non-ionic surfactant and particle in water, surfactant in red round, water in blue round, (left) lower density lignite (right) higher density lignite

## Conclusions

This research focused on surface free energy components of three density lignite samples and the interfacial interaction free energy between low molecular non-ionic surfactant and the lignite surface in water as a medium. The Lifshitz-van der Waals $\gamma^{LW}$ components were 28.58, 22.87 and 20.12 mN/m for -1.45 g/cm$^3$ +1.45-1.80 g/cm$^3$ and +1.80 g/cm$^3$ lignite samples, respectively, which decreased with the increase of the lignite density. However, the hydrophilic indexes $\sqrt{\gamma_s^+}+\sqrt{\gamma_s^-}$ were 2.97, 3.23 and 3.43, which were related to the density positively. Therefore, inorganic oxygen functional groups were more hydrophilic than organic oxygen functional groups. The interfacial interaction free energy results indicated that a non-ionic surfactant had the priority to adsorb on the lower density lignite surface. In addition, the Lewis acid-base interaction free energy played a predominant role in the adsorption interaction. This type interaction intensity increased with the decrease of the reagent hydrophilic index for each density sample. On the other hand, the hydrophilic index of the surfactant was affected by its oxygen functional group types and hydrocarbon chains. Ether bonds and hydroxyl groups were more hydrophilic than ester groups though the same oxygen atoms were maintained in the reagent molecules of TPnB and DOP. In addition, a cyclic hydrocarbon structure led to the stronger hydrophilicity of surfactant. Hence, the low hydrophilic index, regardless of surfactant or lignite, benefited for the Lewis acid-base interaction intensity. However, the Lifshitz-van der Waals interaction intensity showed the positive relationship with the Lifshitz-van der Waals components of the surfactants for the lower and medium density fractions of lignite. However, larger Lifshitz-van der Waals components of the surfactants led to the stronger repulsive intensity for the +1.80 g/cm$^3$ lignite fraction. In conclusion, to increase the adsorption intensity discrepancy between coal-rich and mineral-rich lignite particles, it may provide benefit to increase the Lifshitz-van der Waals component of the non-ionic surfactant.

## Acknowledgements

## References

SARIKAYA M., ÖZBAYOGLU G., 1995, *Flotation characteristics of oxidized coal*, Fuel, 74(2):291-294.

WEN W.W., SUN S.C., 1977, *Electro kinetic study on the amine floatation of oxidized coal*, Transactions of the Society of Mining Engineers of AIME, 262(2): 174-180.

ZHANG H., LIU Q., 2015, *Lignite cleaning in Nacl solutions by a reverse flotation technique*, Physicochemical Problems of Mineral Processing, 51(2): 695-706.

CELIK, M.S., YOON, R.H., 1991, *Adsorption of poly (oxyethylene) nonylphenol homologues on a low ash coal*, Langmuir, 7(8): 1770-1780.

VAMVUKA D., AGRIDIOTIS V., 2001, *The effect of chemical reagents on lignite flotation*. International Journal of Mineral Process, 61(3): 209-224.

ZHANG W., TANG X., *Flotation of lignite pretreated by sorbitan monooleeate*. Physicochemical Problems of Mineral Processing. 2013, 50(2): 759-766.

XIA W., Yang J., 2013, *Reverse Flotation of Taixi Oxidized Coal*, Energy Fuels, 27, 7324-7329.

VAN OSS C.J., 2006, *Interfacial Forces in Aqueous Media*, New York: Marcel Dekker, 161-184.

VAN OSS C.J., OMENYI S.N., NEUMANN A.W., 1979, *Negative Hamaker coefficients*, Colloid and Polymer Science, 257(7): 737-744.

VAN OSS C.J., ABSOLOM D.R., NEUMANN A.W., 1980, *The hydrophobic effect: essentially a van der Waals interaction*, Colloid and Polymer Science, 258(4): 424-427.

CHAU T.T., 2009, *A review of techniques for measurement of contact angles and their applicability on mineral surfaces*, Minerals Engineering, 22, 213-219.

GRUNDKE K., BOGUMIL T., GIETZELT T., JACOBASCH H.J., KWOK D.Y., NEUMANN A.W., 1996, *Wetting measurements on smooth, rough and porous solid surfaces*, Progress in Colloid and Polymer Science, 101, 58-68.

ZOU W., CAO Y., LIU J., LI W, LIU C., 2013, *Wetting process and surface free energy components of two fine liberated middling bituminous coals and their flotation behaviors*, Powder Technology, 246, 669-676.

WANG H., GUO C., FU J., HE Z., LIANG W., CHEN X., ZHUANG C., 2011, *Adsorption behavior of weak hydrophilic substances on low-energy surface in aqueous medium*, Applied surface science, 257, 7959-7967.

IVESON S.M., HOLT S., BIGGS S., 2000, *Contact angle measurements of iron ore powders*, Colloids and Surfaces A: Physicochemical and Engineering Aspects, 166(1-3): 203-214.

LI Z., GIESE R.F., VAN OSS C.J., YVON J., CASES J., 1993, *The surface thermodynamic properties of talc treated with octadecylamine*, Colloid and Interface Science, 156(2): 279-284.

PAINTER P.C., SNYDER, R.W., 1981, *Concerning the application of FT-IR to the study of coal: a critical assessment of band assignments and the application of spectral analysis programs*. Appl. Spectrosc, 35, 475-485.

LIANG Y., TIAN F., LUO H., TANG H., 2015, *Characteristics of coal re-oxidation based on microstructural and spectral observation*, International Journal of Mining Science and Technology, 25, 749-754.